Technical Notes

TECHNICAL NOTES are short manuscripts describing new developments or important results of a preliminary nature. These Notes cannot exceed 6 manuscript pages and 3 figures; a page of text may be substituted for a figure and vice versa. After informal review by the editors, they may be published within a few months of the date of receipt. Style requirements are the same as for regular contributions (see inside back cover).

Analysis of Transonic Integral Equations: Part I—Artificial Viscosity

W. Ogana*
University of Nairobi, Nairobi, Kenya

Introduction

JAMESON[1] showed that the mixed-differencing scheme could be derived by adding an artificial viscosity term to the original differential equation. The artificial viscosity concept has since found wide application in finite-difference methods. Extension to the integral equation is recent and has been confined to the equation involving a decay function.[2,3] In this Note, we use artificial viscosity to solve the two-dimensional transonic integro-differential and integral equations at nodes located throughout the computational domain. To obtain results close to the conservative solutions in finite differences, it is necessary to carry out mixed differencing and to adjust the velocities immediately downstream of the shock point using an interpolation formula in a manner analogous to the proposal by Oswatitsch, as described by Schreier.[4] Computation is carried out for nonlifting parabolic-arc and NACA 0012 airfoils.

Integro-differential and Integral Equations

In conservation form, the two-dimensional-transonic small-disturbance equation, with an artificial viscosity term, may be written

$$\frac{\partial}{\partial x}\left(\phi_x-\frac{1}{2}\phi_x^2\right)+\frac{\partial}{\partial y}(\phi_y)-\frac{\partial}{\partial x}(\mu P)=0 \tag{1}$$

For integral equation methods, Eq. (1) is put in the form

$$\nabla^2\phi = G(x,y) \tag{2}$$

where

$$G(x,y)=\frac{1}{2}\frac{\partial H}{\partial x} \tag{3a}$$

$$H(x,y)=\phi_x^2+2\mu P=u^2+2\mu P \tag{3b}$$

$$P=\Delta x\frac{\partial}{\partial x}\left[\phi_x-\frac{1}{2}\phi_x^2\right]=\Delta x\frac{\partial}{\partial x}\left[u-\frac{1}{2}u^2\right] \tag{3c}$$

$$\mu\begin{cases}1, & \phi_x>1\\ 0, & \phi_x<1\end{cases} \tag{3d}$$

in which Δx is the streamwise grid spacing. Equation (2) is solved subject to appropriate boundary conditions on the body and at infinity. For a normal shock, the following condition should be satisfied

$$\left\langle u-\frac{1}{2}u^2\right\rangle=0 \tag{4}$$

where $\langle\cdot\rangle$ denotes the jump in a quantity across a shock.

Application of Green's theorem to Eq. (2) and subsequent integration by parts yields the transonic integro-differential equation (TIDE),

$$\phi(x,y)=\phi^B(x,y)+\iint_S K_1(\xi-x,\zeta-y)H(\xi,\zeta)\,\mathrm{d}S \tag{5}$$

where ϕ^B and K_1 are defined below. The boundary conditions term is

$$\phi^B(x,y)=\frac{1}{2\pi}\int\left\{\lambda_1F'(\xi)\ln[(\xi-x)^2+y^2]+\gamma(\xi)\left[\frac{\pi}{2}\operatorname{sign}(y)-\arctan\left(\frac{\xi-x}{y}\right)\right]\right\}\mathrm{d}\xi \tag{6}$$

in which $\lambda_1=(\gamma+1)/\pi K^{3/2}$, where K is the transonic similarity parameter, $F(x)$ is the thickness distribution, and $\gamma(x)=u(x,+0)-u(x,-0)$ is the load distribution.

The kernel is defined as

$$K_1(\xi-x,\xi-y)=\frac{x-\xi}{4\pi[(\xi-x)^2+(\zeta-y)^2]} \tag{7}$$

Differentiation of Eq. (5) with respect to x yields the transonic integral equation (TIE)

$$u(x,y)=u^B(x,y)+\nu u^2(x,y)+\iint K_2(\xi-x,\zeta-y)H(\xi,\zeta)\,\mathrm{d}S \tag{8}$$

where $u^B=\partial\phi^B/\partial x$ and $\nu=(1/\pi)\arctan(\lambda)$, in which λ is the height-to-width ratio of the infinitesimal rectangle that surrounds the singularity of the kernel, as described by Ogana and Spreiter.[5]

The kernel is

$$K_2(\xi-x,\zeta-y)=\frac{(\xi-x)^2-(\zeta-y)^2}{4\pi[(\xi-x)^2+(\zeta-y)^2]^2} \tag{9}$$

Numerical Analysis

The computational domain is divided into N rectangular elements, denoted $\Delta_1,\Delta_2,\ldots,\Delta_N$. Let Δ_j have width $2\delta_j$, height $2h_j$, aspect ratio $\alpha_j=h_j/\delta_j$, and center with coordinates (X_j,Y_j). Solutions are obtained at the nodes $Q_1,Q_2,\ldots,Q_N$,

Received March 27, 1987; revision received Nov. 21, 1988.

*Associate Professor, Department of Mathematics. Member AIAA.

where Q_j has coordinates (x_j, y_j). If Δ_j touches the x axis, Q_j is located on the side touching the x axis, such that $x_j = X_j$. But if Δ_j is away from the x axis, Q_j is located at the center of Δ_j.

To give a single description for the numerical solutions of the TIDE and TIE, we let

$$\psi(x,y) = \begin{cases} \phi(x,y) & \text{for the TIDE} \\ u(x,y) & \text{for the TIE} \end{cases} \tag{10a}$$

$$K = \begin{cases} K_1 & \text{for the TIDE} \\ K_2 & \text{for the TIE} \end{cases} \tag{10b}$$

If we apply Eqs. (5) and (8) at Q_i and assume that H is constant within Δj and takes the value at the node, then we obtain the nonlinear system

$$\psi_i = \psi_i^B + \sum_{j=1}^{N} b_{ij} H_j \qquad i = 1,2,\ldots,N \tag{11}$$

where

$$\psi_i = \psi(Q_i), \qquad H_j \equiv H(Q_j),$$

$$b_{ij} = \int_{\Delta_j}\!\!\int K(\xi - x_i, \zeta - y_i)\,\mathrm{d}S \tag{12}$$

The matrix elements b_{ij} may be evaluated by Gaussian quadrature; however, Eq. (12) is straightforward to integrate. The system in Eq. (11) is solved by Jacobian iteration.

Derivatives and Shocks

Solution of Eq. (11) requires evaluating H_j and, thus, determining the derivatives in H. From Eqs. (3) it is obvious that when we solve the TIDE then H is regarded as a function of ϕ_x, but when we solve the TIE it is regarded as a function of u. How the derivatives in H are evaluated is important for solving the flow with shocks.

Define the central difference formula

$$\left(\frac{\partial F}{\partial x}\right)_j = \frac{F_{j+½} - F_{j-½}}{\Delta x} \tag{13}$$

and the backward difference formula

$$\left(\frac{\partial F}{\partial x}\right)_j = \frac{F_j - F_{j-1}}{\Delta x} \tag{14}$$

To solve the TIDE requires evaluation of

$$H_j = (\phi_x^2)_j + 2(\mu P)_j \tag{15}$$

If the node is in a subsonic flow region, the term $(\phi_x^2)_j$ is evaluated using Eq. (13), where we take

$$F_{j\pm½} = ½\,[F_j + F_{j\pm1}] \tag{16}$$

If Q_j is in a supersonic flow region, $(\phi_x^2)_j$ is evaluated using Eq. (14). For the artificial viscosity term $(\mu P) = \mu_j P_j$, we evaluate P_j using Eq. (14) to find

$$P_j = \Delta x\left[1 - \frac{\phi_{j+1} - \phi_{j-1}}{2\Delta x}\right]\left[\frac{\phi_{j+1} - 2\phi_j + \phi_{j-1}}{(\Delta x^2)}\right] \tag{17}$$

If $(\phi_x^2)_j$ is evaluated by central differences throughout, the predicted shock is weak and is located upstream of the correct position. Mixed differencing is, therefore, necessary to produce the appropriate directional bias. In finite differences this is achieved by approximating the derivative $\partial(\mu P)/\partial x$ using Eq. (14) and then evaluating the derivatives in P by Eq. (13). For the TIDE this is not possible, because integration by parts to yield Eq. (5) eliminates one derivative.

The preceding scheme is supplemented with the normal shock condition [Eq. (4)], which may be expressed as

$$u_{s2} = 2 - u_{s1} \tag{18}$$

where u_{s1} and u_{s2} are the velocities upstream and downstream of the shock, respectively. At each iteration, the quantity u_{s1} is determined from Eq. (11), but u_{s2} is determined from Eq. (18).

The preceding procedure alone does not yield the correct conservative solution because there is a slight discrepancy in values immediately downstream of the shock point. This is not confined to the current method, but appears to be characteristic of integral equation methods.[6] To correct the situation, we note that the deviation from the conservative solution vanishes rapidly downstream of the shock point. Let the node Q_s be at the shock point, where the velocity is determined from Eq. (18) and is assumed to be accurate. We choose a node Q_{s+k}, located k rectangles or nodes downstream of the shock point, at which we consider the deviation to be negligible. It is sufficient to choose $k \geq 3$, but larger k gives better results. We use Lagrange interpolation to fit a polynomial through the velocities at Q_s, Q_{s+k} and a suitable number of nodes downstream of Q_{s+k}. From the interpolating polynomial we now estimate the velocities at all nodes between Q_s and Q_{s+k}. This method may be applied through some or all of the iterations. It is analogous to the process described by Schreier[4] and attributed to Oswatitsch. The difference is that Oswatitsch used a parabola to fit the velocities downstream of the shock point, whereas we can fit a higher degree polynomial and, thus, obtain better accuracy.

To solve the TIE requires evaluation of

$$H_j = (u^2)_j + 2(\mu P)_j \tag{19}$$

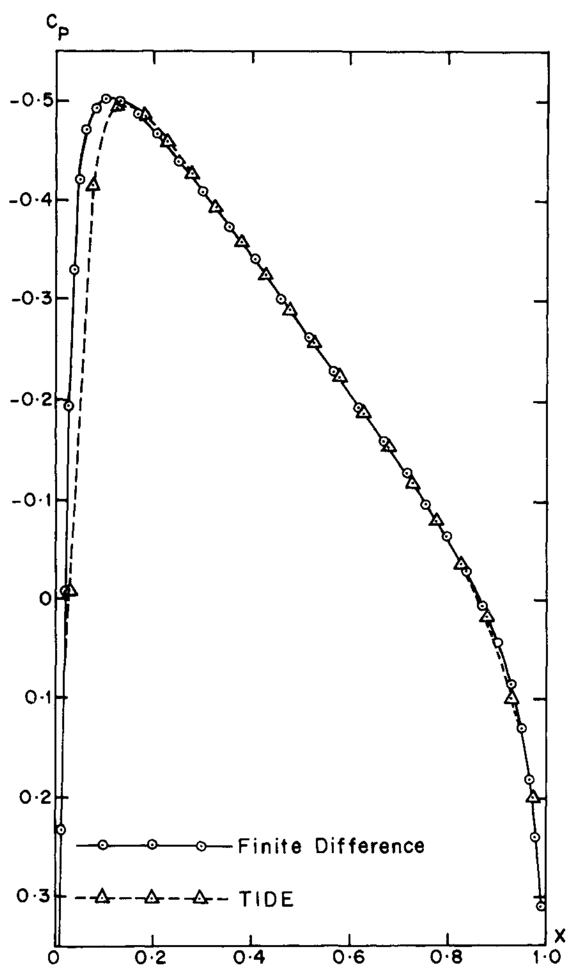

Fig. 1 Coefficient of pressure for NACA 0012 airfoil at $M_\infty = 0.63$.

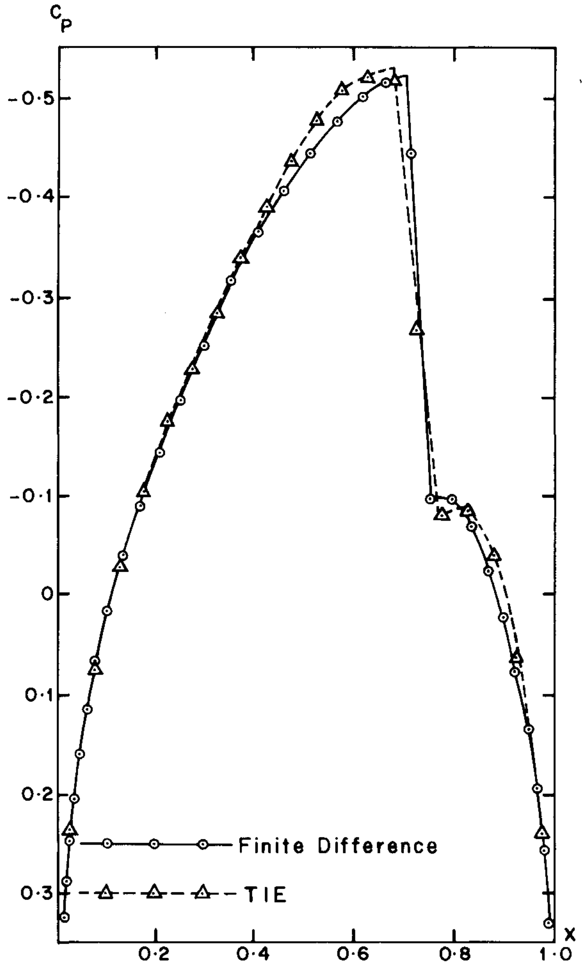

Fig. 2 Coefficient of pressure for a parabolic-arc airfoil of thickness ratio 0.06, at $M_\infty = 0.87$.

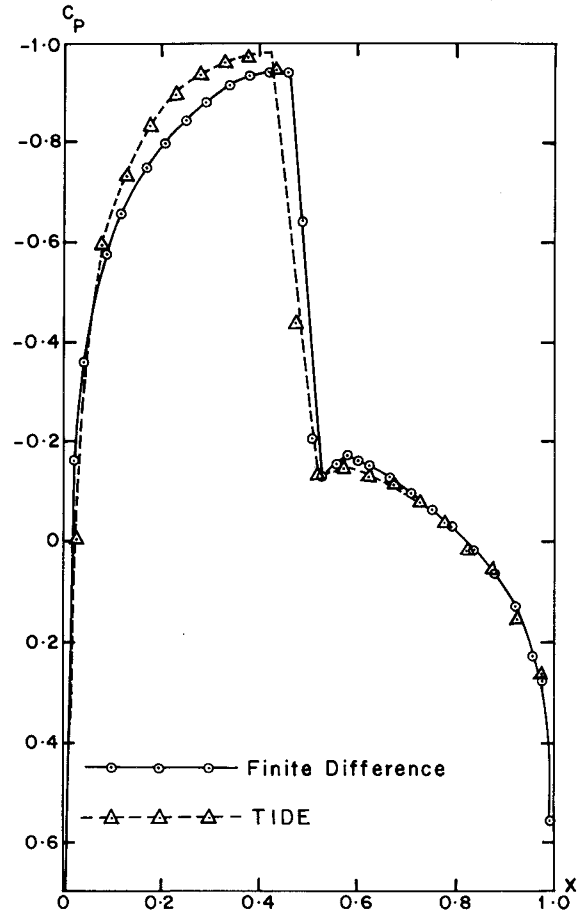

Fig. 3 Coefficient of pressure for NACA 0012 airfoil at $M_\infty = 0.8$.

In order to solve flows with shocks we make a direct extension of the procedure described previously. If Q_j is in a subsonic flow region, we take $(u^2)_j = u_j^2$. But if Q_j is in a supersonic flow region, we take $(u^2)_j = u_{j-1/2}^2$ where $u_{j-1/2}^2$ is determined from Eq. (16). For the artificial viscosity term, the derivative in P is evaluated using Eqs. (13) and (16). Enforcement of the shock condition and adjustment of the velocities just downstream of the shock point are carried out as described for the TIDE.

Results

The computational domain was discretized into four equal horizontal strips, with each strip divided into 50 rectangular elements, not necessarily of equal width. This yielded 200 nodes of which 20, equally spaced, were located on the airfoil. Computation was carried out on a Gould 32 computer. Iteration stopped when the relative error between successive iterates of u was less than 0.01 at all nodes. For adjustment of the velocities immediately downstream of the shock point, a fourth-degree interpolating polynomial was used.

Figure 1 shows the coefficient of pressure plots obtained by solving the TIDE [Eq. (5)] for a NACA 0012 airfoil in subcritical flow. Convergence occurred in four iterations. The coefficient of pressure plots for a parabolic-arc airfoil in supercritical flow, obtained by solving the TIE [Eq. (8)], are shown in Fig 2. The corresponding NACA 0012 airfoil results, obtained from the TIDE, are shown in Fig. 3. Convergence occurred in eight iterations for the parabolic-arc airfoil and 21 for the NACA 0012 airfoil. The finite-difference results in Figs. 1 and 2 are from Ballhaus et al.[7] Those in Fig. 3 are from the Euler equation solution by Jameson.[8] The present results compare favorably with finite-difference solutions despite the relatively small number of nodes used. However, velocities tend to be higher in the supersonic zone, particularly just upstream of the shock. In addition, the NACA 0012 airfoil velocities near the leading edge tend to differ slightly from the finite-difference results partly due to the coarse mesh and to the singularity in the integral, which involves the thickness distribution in Eq. (6). These characteristics have, however, been displayed in other integral equation methods.[2,6,9]

References

[1]Jameson, A., "Computational Fluid Dynamics," VKI Lecture Series, von Karman Institute for Fluid Dynamics, Rhode-St. Genese, Belgium, 1976.

[2]Takanashi, S., "Analysis of Artificial Viscous Transonic Flow," *Proceedings of the 13th Fluid Dynamics Conference,* 1981, pp. 1-11.

[3]Takanashi, S., "A Numerical Solution of the Transonic Integral Equation and its Application to Three-Dimensional Transonic Wing Design," *Proceedings of the 2nd NAL Symposium on Aircraft Computational Aerodynamics,* 1984, pp. 280-291.

[4]Schreier, S., *Compressible Flow,* Wiley, London, 1982, Chap. 6.

[5]Ogana, W. and Spreiter, J. R., "Derivation of an Integral Equation for Transonic Flows," *AIAA Journal,* Vol. 15, Feb. 1977, pp. 281-283.

[6]Spreiter, J. R., "Transonic Aerodynamics – History and Statement of the Problem," *Transonic Perspective Symposium,* NASA Ames Research Center, Moffett Field, CA, 1981, pp. 3-79.

[7]Ballhaus, W. F., Jameson, A., and Albert, J., "Implicit Approximate-Factorization Schemes for the Efficient Solution of Steady Transonic Flow Problems," NASA TM-73202, 1979.

[8]Jameson, A., "Transonic Airfoil Calculations Using the Euler Equations," *Numerical Methods in Aeronautical Fluid Dynamics,* Academic, London, 1982.

[9]Ogana, W., "Solution of Transonic Flows by an Integro-Differential Equation Method," NASA TM-78490, 1978.